Revista Argentina de Clínica Psicológica
2020, Vol. XXIX, N°5, 1909-1917
DOI: 10.24205/03276716.2020.1187

Acceleration Photoplethysmogram using the Long Short-Term Memory Neural Network

JAE MOK AHN[a]

Abstract

Acceleration photoplethysmogram (APG) analysis is widely used to evaluate peripheral vascular status. However, it is difficult to detect the APG parameters that represent vascular health because the signal, which is obtained from the second derivative of a photoplethysmogram (PPG), is characterized by obscure inflection points. Therefore, in this study, we investigated an optimal sequence prediction model for APG signals using the long short-term memory (LSTM) neural networks, excluding the mathematical detection algorithm of five inflection points. To build an APG LSTM model, we used 5000 APG training datasets and 1000 validation datasets to fit the stacked LSTM model. APG signals were obtained from six subjects, who had no atherosclerosis in the blood vessels. The 1000-training data per a subject were generated with different magnitudes and periods representing the time interval between two heartbeats. An input training data length of 150 was used. Stacked LSTM for the number of hidden layers showed mean loss (0.000487 for 10 cells, 0.000111 for 100 cells, 0.000200 for 200 cells, and 0.000035 for 300 cells), resulting in excellent prediction in differentiating the characteristics of the APG signal. The results indicate that an LSTM neural network with over 200 memory cells and four hidden layers for APG signal analysis can be used to assess vascular status changes and stiffness in the peripheral blood vessel wall. A limitation that various conventional detection methods have showed could be resolved through an introduction of a deep learning methodology.

Keywords: acceleration photoplethysmogram, atherosclerosis, blood vessel, long short-term memory, neural network.

1. Introduction

Acceleration photoplethysmogram (APG) analysis is of interest to clinicians and biomedical engineers. APG provides information that can quantify vascular status through an algebraic calculation of five inflection waves (a, b, c, d, and e peaks) in its signal. A vascular index using these five waves represents cardiac stroke, vascular compliance, vascular elasticity, ejection fraction, arterial pulse wave feature, and residual volume fraction in the peripheral blood vessel vein [1-4]. The APG waveform is derived from the second derivative of the photoplethysmogram (PPG), making its parameters more detectable than those of PPG. The PPG signal is generated when a 660-1100 nm wavelength light-emitting diode (LED) transmits light through a subject's index finger while a photodiode detects absorption on the opposite side for every cardiac cycle [5].

The PPG waveform includes cardiovascular-related information that, depending on age and specific diseases, is particularly useful for diagnosis and treatment [6-9]. However, the quality of the PPG signal is susceptible to measurement position, ambient environment, patient posture, changes in the autonomic nervous system, and measurement time. Therefore, feature extraction from an APG waveform generated by the second derivative of an inherently noisy PPG is difficult. Mathematically, a derivative of the PPG signal is accompanied by noise amplification owing to slope calculation characteristics, as shown in Fig. 1. Therefore, to extract APG parameters, studies have proposed various methodologies, including multimodal biometric recognition, use of a fourth derivative, pulse contour analysis, complete removal of motion artifacts, and direct morphological analysis using frequency-domain estimates [10-13]. There is still no robust method to accurately detect the five

[a]School of Software, Hallym University, Chuncheon, Gangwon-do, Republic of Korea
Corresponding author: Prof. JAE MOK AHN, Ph.D.
School of Software, Hallym University, 1 Hallymdaehak-gil, Chuncheon, Gangwon-do, 24252 Republic of Korea
Tel +82 033 248 2347 Fax +82 033 242 2524 Email : ajm@hallym.ac.kr

inflection waves as APG parameters for calculating a vascular index to predict vascular age or vascular aging rate.

However, with the increasing popularity of machine learning technology, a new study used a deep learning algorithm, and investigated measurement of blood pressure or hypertension stratification using the PPG signal itself without signal extraction [14,15]. The machine learning approach has been used for detection of atrial fibrillation from PPG time series, which produces morphological descriptors [16,17]. All PPG-based machine learning algorithms have been associated with the classification of blood pressure and electrocardiogram signals. However, there are no studies on the direct use of raw APG signals for training deep learning models to identify APG characteristics according to vascular status with aging.

Therefore, we investigated an optimal deep learning model, the long short-term memory (LSTM) neural network with four hidden layers, in terms of the number of cells to minimize the loss involved in using raw APG data. Based on a deep learning model (LSTM), classification of APG type representing vascular aging information was carried out. LSTM is an advanced model of a recurrent neural network (RNN) architecture with memory to classify, process, and predict time series. The main reason that LSTM was chosen over the Markov model and other sequence learning models is to provide good results in various sequence lengths. To predict the sequence of the APG data after an arbitrary interval, a deep learning model with memory (such as LSTM) is required.

This study fitted the LSTM model with 5000 sequences of APG data and input different types of APG waveform ranging from type A to F. The 1000 validation datasets were used to compare the predicted and expected APG sequences. The two sequences are plotted on the sample chart. The results indicate that the stacked LSTM with 256 memory cells would be useful for predicting the next APG signal and examining the relationship between physical age and APG signals without using direct APG parameters obtained from a conventional detection algorithm.

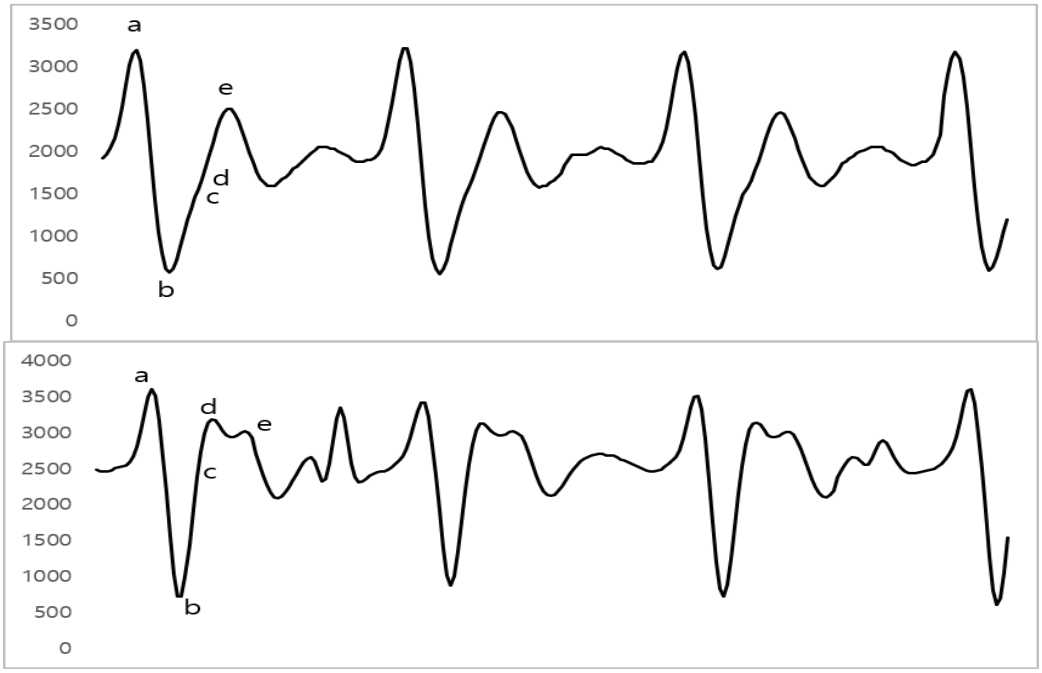

Figure 1. **Acceleration plethysmogram (APG) waveform with five inflection features: (top) APG waveform without motion artifacts, and (bottom) APG waveform with motion artifacts.**

2. Material and methods

2.1 Data Preparation

Our study included six subjects in good health. PPG signals using SpO2 sensor embedded into polysomnography (PSG) were measured at a sampling frequency of 200 Hz, using a computerized polysomnographic device (Nox-A1, Nox Medical Inc. Reykjavik, Iceland). APG signals using a Canopy9 RSA pulse analyzer (TAS9VIEW, IEMBIO Co. Ltd, Chuncheon, South Korea) were obtained from the second derivative of the PPG signals with a 1D data sequence. For both the training and input data, to fit and predict the LSTM model, APG signals were sampled down to 100 Hz

to reduce the training time and converted to a 3D data frame to input an LSTM neural network.

In the real world, because various cardiac cycles ranging from 30 bpm to 200 bpm are required for training the input data, all APG signals were created by using a random function to change the heart period step by step. In addition, the APG amplitude was simultaneously controlled to 50 % of the maximum amplitude by decrements of 1 %. Six different types of APG waveforms were selected from the PSG data to change compliance and elasticity in a peripheral blood vessel, which means that six subjects are found with individual types of blood vessels from type A to type F in Fig. 2. Finally, all the APG signals were standardized with a standard deviation (STD) of 1.0 and mean of 0.0. This is owing to the activation function of the LSTM being the sigmoid function for the input gate and tanh function for the input modulation gate; it has a range of [-1.0, 1.0]. For the training and test data, 5000 and 1000 APG sequences with an individual dataset of 150 (corresponding to data length) were prepared, respectively. A data length of 150 was considered as it includes at least two or three cardiac cycles in a single frame.

This study adhered to the tenets of the Declaration of Helsinki and was approved by the Institutional Review Board of Hallym Medical University Chuncheon Sacred Hospital (IRB No. 2020-03-022). Additionally, the need for written informed consent was waived because this study was designed to be retrospective.

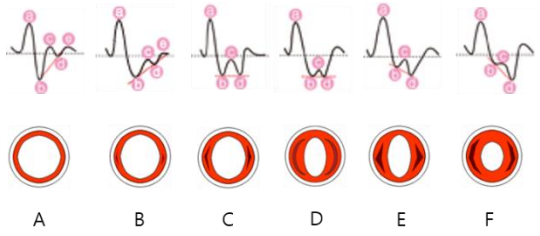

Figure 2. **Six types of APG waveform indicate the corresponding vascular status from A type, the best case, to F type, the worst case.**

2.2 Long Short-Term Memory (LSTM)

The stacked LSTM network comprises many layers of neurons, which have recurrent connections so that the internal state of the previous layer from the previous time step is memorized to uniquely formulate an output. An LSTM layer consists of a set of recurrently connected blocks known as memory cells. Each memory cell contains one or more recurrently connected memory cells and three multiplicative gates. Each memory cell consists of three sigmoidal functions and one hyperbolic tangential function. The memory cells have weight parameters, which are used to weight input for the X[t] time step, output from the last X[t+n] time step, and internal state h[n] used in the calculation of the output for this time step. These weight parameters control the information flow as APG sequence data in the memory cell. The LSTM neural network interacts only with the memory cell via three gates, which are the key to the memory cell of the LSTM, as shown in Fig. 3. Fig. 3 illustrates how each memory unit in LSTM is composed with three gates: forget, input, and output gates.

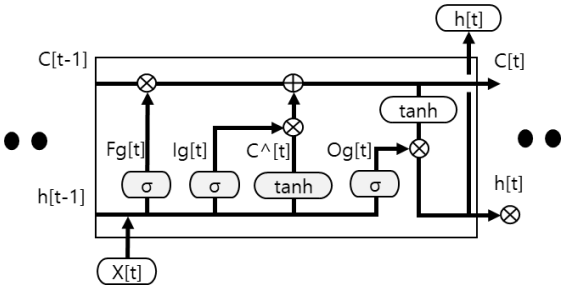

Figure 3. **Multiple memory blocks in an LSTM contain four interacting layers (in gray): three sigmoidal functions and one hyperbolic tangential function.**

The forget gate (Fg[t]) decides which APG input data to abandon from the memory cell, input gate (Ig[t]) decides which APG input data to update the internal cell state with, c[t] (Fg[t]), and output gate (Og[t]) decides what to output based on the input, X[t] and internal cell state, c[t].

For new information to be stored in the internal cell state, two cells are used. A sigmoid cell for input gate, Ig[t], that decides which APG data points will be updated, and a tanh cell creates a vector of new candidate data points, C^[t], which is added to the internal cell state. To update the old cell state, C[t-1], into the new cell state C[t], we multiplied the old internal state, C[t-1] by forget gate, Fg[t], and added Ig[t]*C^[t]. A sigmoid cell of Fg[t] outputs a number between 0 and 1, where a 1 represents the keeping internal state whereas a 0 represents the discarding internal state. The mathematical equations among all gates and weights are as follows

$$Fg[t] = \sigma(W_f \cdot [h[t-1], X[t]] + b_f) \quad (1)$$

$$Ig[t] = \sigma(W_i \cdot [h[t-1], X[t]] + b_i) \quad (2)$$

$$C\hat{}[t] = \tanh(W_C \cdot [h[t-1], X[t]] + b_C) \quad (3)$$

$$C[t] = Fg[t] * C[t-1] + Ig[t] * C\hat{}[t] \quad (4)$$

$$o[t] = \sigma(W_o \cdot [h[t-1], X[t]] + b_o) \quad (5)$$

$$h[t] = o[t] * \tanh(C[t]) \quad (6)$$

where σ and h are the activation function of

sigmoid and hidden layer, respectively. A b and W represent the initial bias value and weight matrix, respectively.

We built a stacked LSTM that has four hidden layers, where each layer contains multiple memory cells. Fig. 4 shows a stacked LSTM architecture in which an LSTM layer above provides an APG sequence output to the LSTM layer below. There are four layers which have the number of each memory cell with 256, 256, 128, and 64. Because the depth of the network was more important than the number of memory cells, we investigated stacked layers. The linear activation function was used for the output prediction, and the mean absolute error (MAE) loss function and Adam implementation of the gradient descent optimization algorithm were used. The entire work was carried out using Python application program.

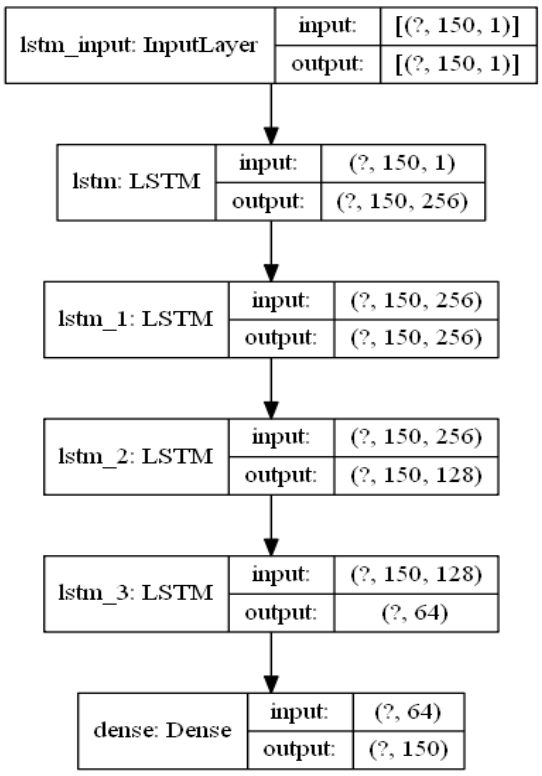

Figure 4. **A stacked LSTM architecture with 150 input time length and four hidden layers for prediction of APG signals.**

2.3 LSTM Parameters

The time steps of the input APG sequence are 150 with the matrix of (150,1), and each time step should have a single characteristic length. For the first LSTM layer in the calculation of parameters, the output length is 256 for each time step due to memory cells of 256, obtaining the matrix of (1,256). Each LSTM block consists of the forget gate, internalcell state gate, and output gate, such as equations (1), (4) and (5), respectively. The length of $[h[t-1], X[t]]$ in equation (1) is 257 due to the contribution of each time step and the cell number of 256 for the first layer (1+256), resulting in the matrix of (1,257). Therefore, the matrix of weight, W_f, is (257,256), and the bias matrix, b_f, must be the matrix of (1,256) from 256 cells as well. Thus, a total number of parameters generated by the forget gate alone is 66,048 (257*256+256). The same goes for the internal cell state gate in the calculation of parameters, which is double the number of forget parameters, as there are no additional parameters for sigmoid and tanh functions in the matrix calculation. Therefore, the internal cell state gate generates 132,096 (66,048*2). For the output gate, equation (5) is the same as equation (1) that the number of parameters has 66,048. Taken together, a total number of parameters combined with three gates lead to 264,192 for the first LSTM layer, as shown in Table 1. The same calculation method could be applied to the second, the third, and the fourth LSTM layer, resulting in trainable parameters of 1,045,782. The last layer expresses the fully connected layer, with 64 cells plus 1 bias and the characteristic length of output, 150.

Table 1. **Parameters of four hidden layers for LSTM neural network.**

Layer (type	Output Shape	Param#
lstm (LSTM)	(None, 150, 256)	264,192
lstm_1 (LSTM)	(None, 150, 255)	525,312
lstm_2 (LSTM)	(None, 150, 128)	197, 120
lstm_3 (LSTM)	(None, 64)	49,408
Dense (Dense)	(None, 150)	9,750
Total params: 1045,782		
Trainable params: 1045,782		
Non-trainable params: 0		

1. Results

We investigated the behaviour of the stacked LSTM model by reviewing its prediction performance over 100 epochs and one batch size. During the compilation of the model, a trace of the loss and other metrics were displayed, as shown in Fig. 5. To measure the accuracy of each epoch, 1000 validation APG datasets with 150-time steps was created to diagnose the behaviour of the stacked LSTM model. An increase in epochs resulted in an exponential drop in loss for the validation APG dataset (Fig. 5). The separate validation APG datasets were intentionally manipulated to combine motion artifacts. The result suggests that

performance on the APG train set and validation set continued to improve simultaneously from a plot where the train loss as well as validation loss sloped down.

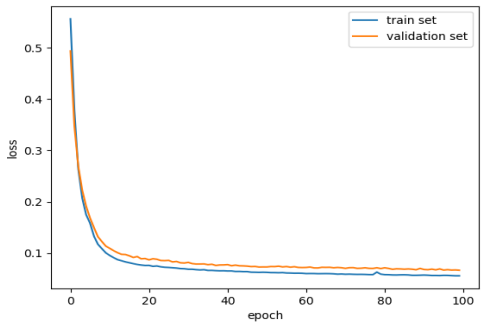

Figure 5. **Plot of the losses in terms of APG training and validation datasets.**

However, the performance of the model demonstrated that the training loss was lower than the validation loss. Using these results, we confirmed that further improvements, such as more training datasets and accurate measurement of APG datasets, are possible for an optimal development of the LSTM model. To resolve this underfit model, the performance was improved by increasing the number of training epochs, the memory cells, and the stacked layers.

Fig. 6 shows different performances of the model by increasing the number of memory cells according to [10, 100, 200, 300] array with 100 training epochs. A box and whisker plot were generated to evaluate the distribution of model skill according to the number of memory cells. The optimal number of memory cells for stacked LSTM architecture cannot be precisely determined without adequate APG training datasets. A sharp decrease in loss was found at over 200 memory cells, where the number of an optimal memory cell of 256 could be determined for our study.

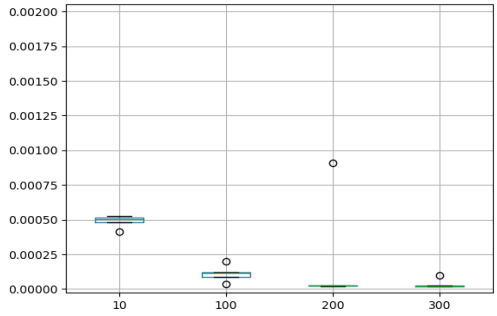

Figure 6. Box and whisker plots of the results of tuning multiple memory cells [10, 100, 200, 300].

Therefore, we tested a group of different memory cells in LSTM hidden layers. While the number of memory cells is changed from 10 to 300, the stacked LSTM model was repeated five times. Summary statistics of the results for each number of memory cells after five repeats are listed in Table 2.

Table 2. **Statistics of the results showing the performance of the stacked LSTM model for building an optimal model. *STD: standard deviation.**

Memory Cells	10	100	200	300
Repeat	5	5	5	5
Mean	0.000487	0.000111	0.000200	0.000035
*STD	0.000045	0.000060	0.000397	0.000034
Min	0.000413	0.000034	0.000022	0.000018
25%	0.000479	0.000086	0.000023	0.000019
50%	0.000502	0.000117	0.000023	0.000020
75%	0.000515	0.000121	0.000025	0.000024
Max	0.000526	0.000198	0.000910	0.000096

Minimal STD represents architecture suitability, which provides a consistent prediction in response to an input with a small change in amplitude. The STDs for 10, 100, 200, and 300 of memory cells were 0.000045, 0.000060, 0.000397, and 0.000034, respectively. In the case of over 250 cells, the STD is expected to be approximately zero. Therefore, for our application, four hidden LSTM layers with memory cells of 256 based on the performance predicted through five repeats were proposed.

The predicted and expected sequences for APG signals using the proposed model are plotted for comparison, as shown in Fig. 7. To evaluate how much two the APG sequences differ, the mean squared error (MSE) percentage that measures the average difference between the expected values (yhat) and predicted value (y) was calculated using the following equation.

$$MSE(\%) = \frac{1}{N}\sum_{i=1}^{N}(y_i - yhat_i)^2 * 100 \quad (7)$$

The MSEs (%) for 60, 120, 180, and 240 bpm were 1.49764, 4.27263, 4.03666, and 4.47466, respectively. The APG with a slow heart rate was more accurate than that with a fast heart rate. Taken together, the prediction appears to be a reasonable fit for the expected APG sequence. Prior to the implementation of the fit model in some machine learning algorithms, the APG dataset for sequence prediction problem must be standardized when training a stacked LSTM recurrent neural network, because APG signals have input values with differing scales. We rescaled the distribution

of values so that the mean value was 0 and the STD from subtracting the mean value was 1. As a result, a learning speed and efficiency for the proposed LSTM architecture were improved.

The conventional method that extracts five inflection points on an APG signal has an inherent problem in detecting a heart rate with more than 100 bpm. Among the five APG parameters, the c and d peaks could not be easily extracted because their positions in the time series were too close. In addition, it is impossible to detect APG parameters for APG signals with motion artifacts. However, a machine learning-based APG classification method for monitoring a vascular status could identify the characteristics of APG waveforms directly without measurements of APG parameters regardless of the heart rate. The stacked LSTM model could predict the degree to which APG signals contain motion artifacts as a value of the MSE (%). The decision to run the model for the APG signals being measured was based on the MSE (%), with the running model stopped when the MSE was greater than 5 %.

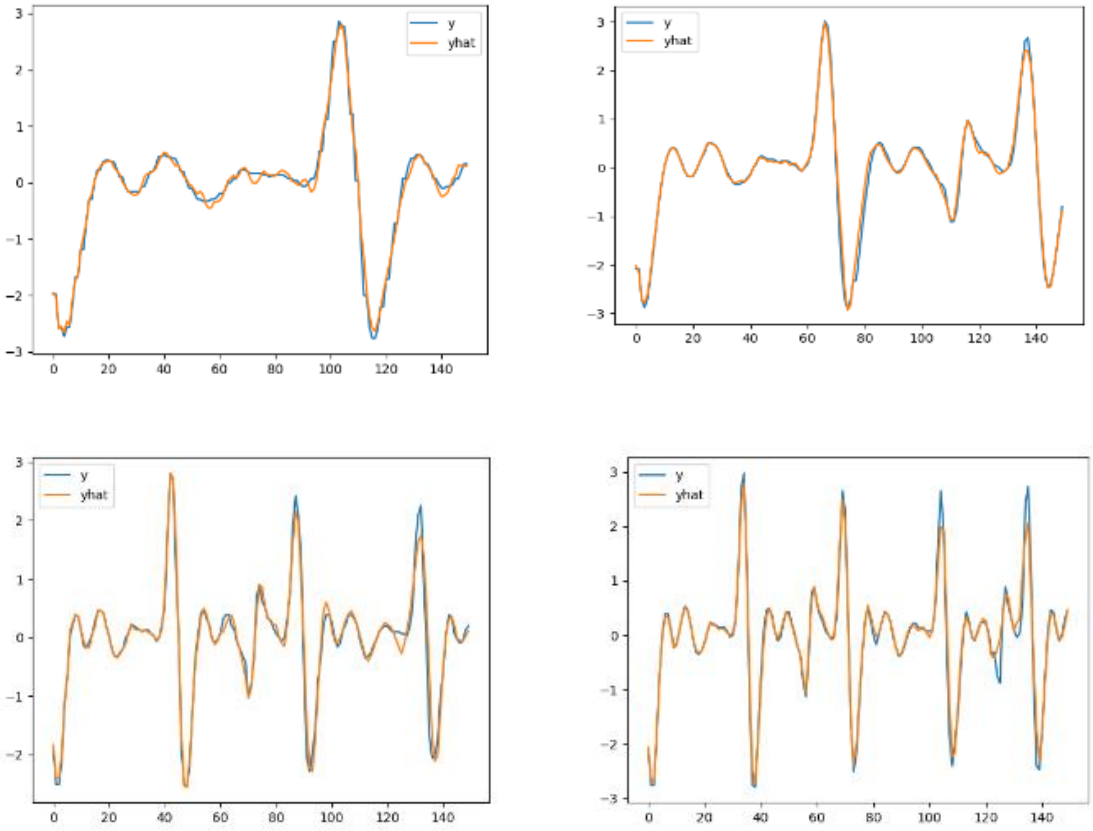

Figure 7 Expected (y) and predicted (yhat) results according to four different cardiac cycles.

Fig. 8 shows that six types of vascular health status obtained based on APG waveforms were predicted through a deep learning model, ranging from type A for the best status to type F for the worst status. Differentiating type E from F through a conventional detection method of APG parameters is technically difficult because the distance between two near-positions is very close to each other even without motion artifacts. In addition, as the distinction between type C and D is not clear, a traditional method made it difficult to distinguish them. A little change in subject's movement during measurements may invalidate the test, resulting in a restart for a new test. However, with a deep learning algorithm, such as an LSTM neural network, these shortcomings were resolved when six types of signal feature representing health of various blood vessel were fed to the stacked LSTM with over 5000 APG sequences. The bottom panel showed that type E and F were correctly predicted when validation data of APG waveform was inputted to the stacked LSTM model. For elderly people aged 70 or over who have suffered from atherosclerosis in a peripheral blood vessel [18,19], APG waveform of type F obtained from a finger index is characterized as a difficult extraction of APG parameters, but it was well predicted. The type B waveform showed

slighter errors than those of other types around the middle location. To minimize these errors, many more training data representing features of type B are required.

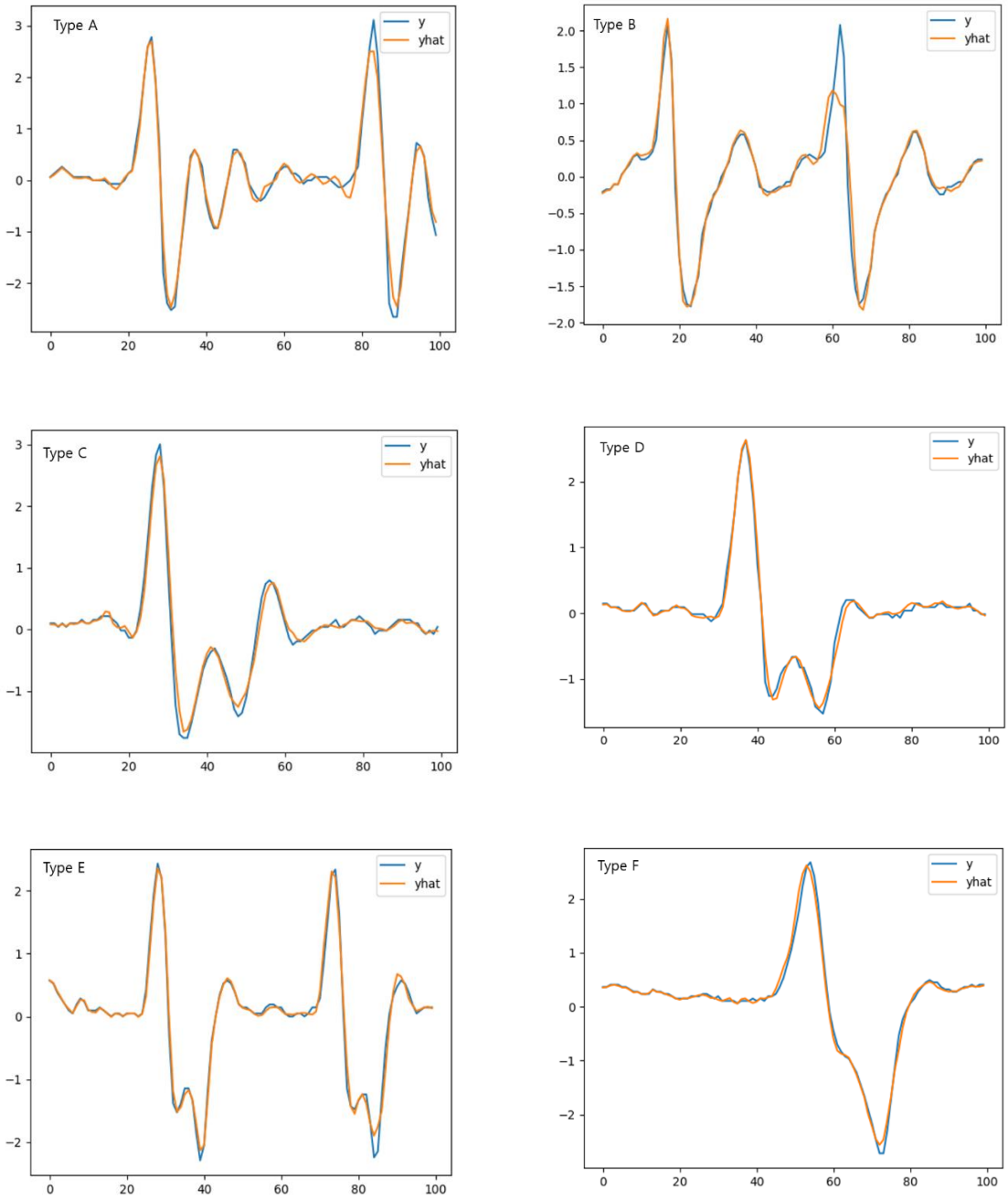

Figure 8 Expected (y) and predicted (yhat) results regarding all vascular types; type A, B, C, D, E, and F.

2. Discussion

This paper proposed an LSTM neural network model for predicting vascular health based on the APG waveform, where the one-dimensional datasets of APG signals in the time series were used as input data. The stacked LSTM model with four hidden layers was constructed after five repetitions for APG sequence prediction. Each hidden layer from input layer to the fourth layer was composed of 256, 256, 128, and 64 for the number of the memory cells, respectively. A stacking LSTM model has not been introduced to APG waveform-based parameter classification before. To build the input data, 5000 APG standardized training data from individual subjects, which included changes in both the amplitude and cardiac cycle, were prepared. It

took approximately eight hours to completely train the model using a notebook computer with Intel® Core™ i5-8250U@1.6GHz without a graphic processing unit. We achieved remarkable results showing no significant difference between the predicted value (y) and expected value (yhat) in less than 5 % of MSE, regardless of the level of heart rate. In addition, we showed that the relationship between the APG waveform and vascular index could be learned by a stacked LSTM neural network architecture without any extractions of the five APG waves, which are difficult to detect owing to the inherent noise characteristics. The performance of the stacked LSTM neural network was satisfactory in terms of the STD of the loss. However, many more APG training datasets that consider the characteristics of signal noise are necessary to meet all various vascular statuses. With a specific number of training datasets including motion artifacts, we evaluated the possibility that the stacked LSTM with four hidden layers could be applied to an APG study that predicted vascular aging. In the future, an LSTM neural network would be further applied to predict the degree of obstructive sleep apnoea during sleep from the relationship between vascular status and magnitude of APG signals, which have never been attempted before.

Acknowledgments

This work was supported by the Hallym University Research Fund (HRF-202010-010).

Disclosure

The authors have no financial disclosures to report. The author reports no conflicts of interest in this work.

References

[1] Criado E, Farber M.A., Marston W.A, et al. (1998). The role of air plethysmography in the diagnosis of chronic venous insufficiency. *Journal of Vascular Surgery*. 27, 660-670.

[2] Anderson F.A. (1984). Impedance plethysmography in the diagnosis of arterial and venous disease. *Annals of Biomed Engineering*. 12, 79-102.

[3] Shabani Varaki E., Gargiulo G.D., Penkala S, et al. (2018). Peripheral vascular disease assessment in the lower limb: a review of current and emerging non-invasive diagnostic methods. *Biomedical Engineering Online*. 17(1), 61-88.

[4] R.J. Whitney. (1953). The measurement of volume changes in human limbs. *Journal of Physiology*. 121(1), 1-27.

[5] Samah Alharbi, Sijung Hu, David Mulvaney, et al. (2019). Oxygen saturation measurements from green and orange illuminations of multi-wavelength optoelectronic patch sensors. *Sensors.* 19(1), 118-135.

[6] S. Rosfors, L.M. Persson, L. Blomgren. (2014). Computerized venous strain-gauge plethysmography is a reliable method for measuring venous function. *European Journal of Vascular and Endovascular Surgery.* 47(1), 81-86.

[7] Dezotti N.R.A., Dalio M.B., Ribeiro M.S., et al. (2016). The clinical importance of air plethysmography in the assessment of chronic venous disease. *Journal of Vascular Brasileiro.* 15(4), 287-292.

[8] P.T. McCollum, S.T. Stanley, P. Kent, et al. (1988). Assessment of arterial disease using digital systolic pressure measurement. *Annals of Vascular Surgery*. 2(4), 349-351.

[9] M.S. Whiteley, A.D. Fox, M. Horrocks. (1998). Photoplethysmography can replace hand-held Doppler in the measurement of ankle/brachial indices. *Annals of Royal College of Surgeons of England*. 80(2), 96-98.

[10] Khairul Azami Sidek, Nur Khaleda Naili Kamaruddin, et al. (2018). The study of PPG and APG signals for biometric recognition. *Journal of Telecommunication, Electronic and Computer Engineering*. 10(1), 17-20.

[11] Jae Mok Ahn. (2017). New aging index using signal features of both photoplethysmograms and acceleration plethysmograms. *Healthcare Informatics Research.* 23(1), 53-59.

[12] Chellappan K., Ali M.M., Zahedi E. (2008). An age index for vascular system based on photoplethysmogram pulse contour analysis. *Proceedings of 4th Kuala Lumpur International Conference on Biomedical Engineering.* 125-128.

[13] Krishnan R., Natarajan B.B., Warren S. (2010). Two-stage approach for detection and reduction of motion artifacts in photoplethysmographic data. *IEEE Transitions on Biomedical Engineering*. 57(8), 1867-1876.

[14] Radha M. (2018). Wrist-worn blood pressure tracking in healthy free-living individuals using neural networks. *arXiv preprint arXiv.* 1805.09121.

[15] Yongbo Liang, Zhencheng Chen, Rabab Ward, et al. (2018). Photoplethysmography and deep learning: Enhancing hypertension risk stratification. *Biosensors (Basel)*. 8(4), 101-114.

[16] Tania Pereira, Nate Tran, Kais Gadhoumi, et al. (2020). Photoplethysmography based atrial fibrillation detection: a review. *npj Digital Medicine*. https://doi.org/10.1038/s41746-019-0207-9.

[17] Shashikumar S.P., Shah A.J., Clifford G.D, et al.

(2018). Detection of paroxysmal atrial fibrillation using attention-based bidirectional recurrent neural networks. *In KDD '18 Proc. Of the 24th ACM SIGKDD International Conference on Knowledge Discovery & Data Mining*. 715-723.

[18] B. Niranjana Krupa, Kunal Bharathi, Manjunath Gaonkar, et al. (2017). Multiclass classification of APG signals using ELM for CVD risk identification: A real-time application. *The 16th International Conference on Biomedical Engineering*. 32-37.

[19] Jeom Keun Kim, Jae Mok Ahn. (2018). New marker for vascular health based on the Poincare plot analysis using acceleration plethysmogram. *International Journal of Applied Engineering Research*. 13(21), 15417-15423.